WIDMANSTÄTTEN PATTERN GROWTH IN IMPACTED, MANTLE-STRIPPED IRON METEORITE PARENT BODIES. R. J. Lyons[1], F. J. Ciesla[1], and N. Dauphas[1,2], [1]The Department of the Geophysical Sciences, The University of Chicago, Chicago, Illinois (rjlyons@uchicago.edu), [2]Origins Laboratory and Enrico Fermi Institute, The University of Chicago, Chicago, Illinois.

Introduction: The Widmanstätten pattern in iron meteorites is a direct reflection of the thermal evolution of their parent bodies. This cross-stitched pattern developed from the exsolution of kamacite (α, body-centered cubic) from taenite (γ, face-centered cubic) as the iron cooled. This growth is temperature dependent, allowing the observed grain sizes and Ni-concentrations to be compared to numerical models of grain growth and Ni diffusion to determine the cooling rate that the iron sample experienced.

To date, models of Widmanstätten pattern formation have set the cooling rate as constant throughout the temperature ranges where mineral growth occurs [1-3]. However, it is possible that cooling rates varied, at times significantly, as the patterns developed. For example, the IVA and IVB iron groups appear to have cooled very rapidly, possibly because they sample the cores of parent bodies whose mantles were stripped away in a hit-and-run impact [2]. While such cores would cool rapidly, with some regions reaching rates of 10^3-10^4 °C/Myr, the cooling rates that a given sample experienced would vary by factors of a few to nearly an order of magnitude through the temperature range that the Widmanstätten pattern formed. To date, it has not been investigated how the pattern would be affected given non-constant cooling rates or how closely the inferred constant cooling rates compared to those the sample actually experienced. Here we investigate the effects of non-constant cooling rates on iron meteorites and discuss the implications for the thermal histories of their parent bodies.

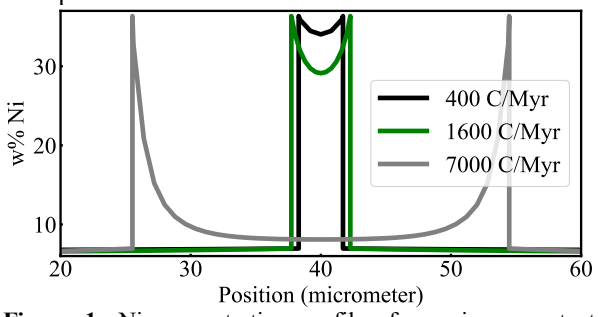

Figure 1: Ni concentration profiles for various constant cooling rates with an impingment length of 40 microns and material properties the same as Gibeon. In each case, the taenite half-width and central Ni concentration vary.

Widmanstätten Pattern Formation Model: We have modified the 1D Ni diffusion model described in [3] which utilizes a front-tracking, fixed finite-difference grid methodology described by [4]. The phase diagram of kamacite and taenite used here is described in [2]. Fig. 1 illustrates the Ni concentration profiles that result from our Widmanstätten pattern formation model. We set the initial distance between kamacite nucleation sites (impingment length) in these runs to 40 microns and material properties the same as the IVA meteorite Gibeon. A given constant cooling rate changes the final shapes of the curves. Faster cooling rates yield larger taenite half-widths (distance between the kamacite-taenite boundaries) and lower central Ni concentrations.

Constant Cooling Rates: In order to verify our model, we reproduced the Wood diagrams of several meteorites as reported in [2]. A Wood diagram plots the central Ni concentration vs. the half-width of the taenite band of a given Widmanstätten pattern. A curve predicting the relationship between these two quantities for a given constant cooling rate can be determined by varying the impingement length at the beginning of each simulation. With such a plot, the cooling rate of a given iron meteorite can be estimated by measuring these values and comparing to the model curves. Fig. 2 shows model results for cooling rates ranging from 400 to 7000 °C/Myr, assuming the Gibeon meteorite composition. The colored lines are those reported in [2] and the gray lines are those from this work. We find there is good agreement between the models.

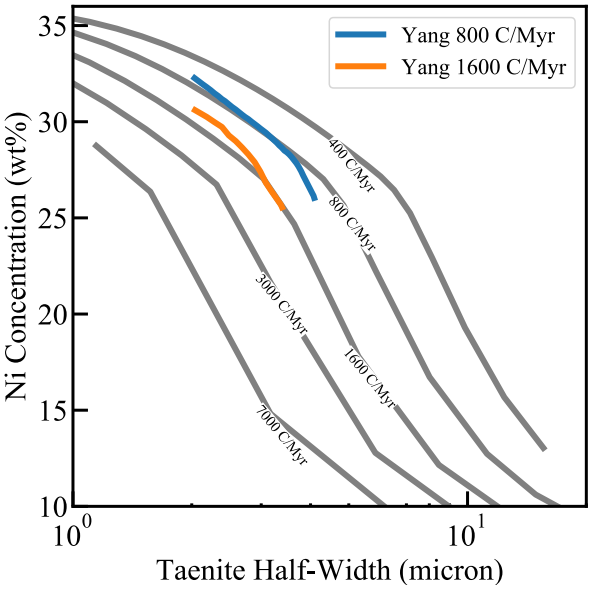

Figure 2: Wood diagram of the IVA iron meteorite Gibeon as determined in [2], colored curves, and our model, gray curves. We find good agreement between the two models.

Mantle-Stripped Cooling Rates: We tracked the thermal evolution of a 150 km radius mantle-stripped iron core using a 1D conductive code [6] with the same parameters as determined by [2] for the IVA parent body. Fig. 3 shows the cooling rates that materials at different depths over the temperature range that the Widmanstätten pattern forms. The cooling rate in a stripped iron body not only will be a function of depth (faster near the surface, slowest at the center) but also temperature, cooling more quickly at high temperatures and more slowly at low. At 0.97R, the cooling rate decreases from 7000 to 3000 °C/Myr over the Widmanstätten pattern growth temperature range of Gibeon. Similarly, at a depth of 0.9R, the cooling rate decreases from 800 to 400 °C/Myr.

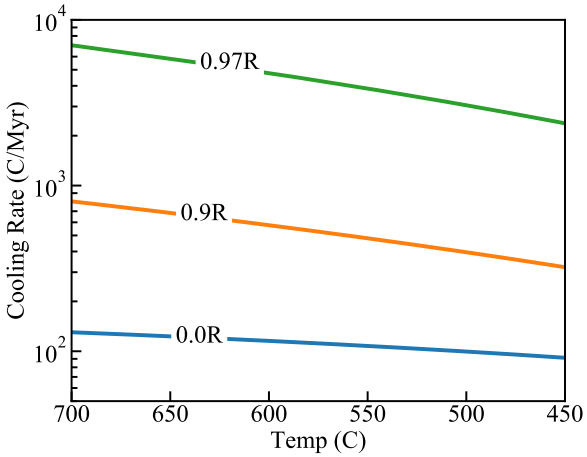

Figure 3: The cooling rate at a given temperature for three depths within a 150 km radius mantle-stripped iron core. The temperature range shown here corresponds to the range over which the Widmanstätten pattern forms.

We ran a suite of simulations using these thermal profiles in order to quantify the relationship between taenite half-width and Ni-concentration that would develop in the cooling iron, again using the same parameters as the Gibeon meteorite. Fig. 4 shows the predicted curves for the depths shown in Fig. 3 alongside curves of constant cooling rate presented in Fig. 2. We see in each case the mantle-stripped curves do not match the constant cooling rate curves, instead following some or crossing them at various locations in the plot. In particular, we find that half-width-Ni concentration relationships agree well with the rapid, constant cooling rates a sample experienced at the beginning of Widmanstätten patterns growth when half-widths are large. Conversely, the narrower half-widths would record a half-width-Ni relation similar to those predicted for the slower cooling rates a sample experienced near the metallographic cooling closure temperature.

Thus, systematic variations between data and constant cooling model predictions may be indicative of changes in the cooling rates for a given sample. As models predict constant cooling rates for iron in differentiated planetesimals, variations like these could be signs that a given meteorite parent body experienced impacts early in its history that affected the thermal evolution of the iron [2,5].

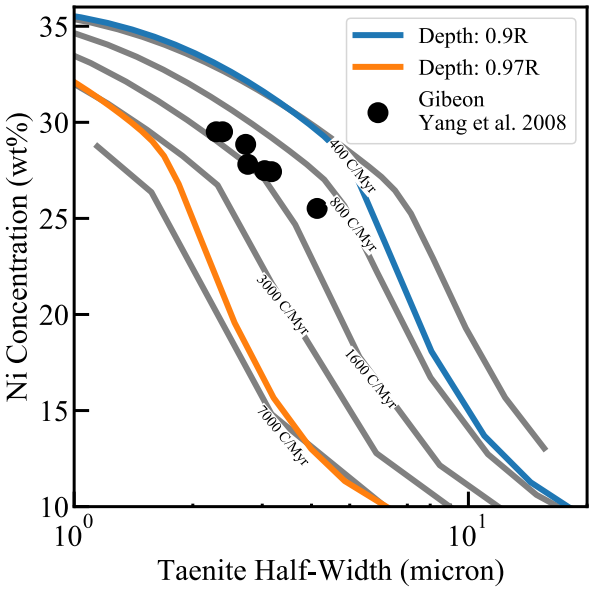

Figure 4: Wood diagram of constant cooling rates (gray) and mantle-stripped iron body at two depths. In each of the non-constant cooling rate cases, the curves transitions between two constant cooling rate curves.

The measurements for the Gibeon meteorite, as reported in [2] and plotted in Fig. 4, do not span a large enough range of taenite half-widths to make a determination if it is following a constant cooling or a mantle-stripped curve. However, the measurements are suggestive of deviations from the 1600 °C/Myr cooling rate outside of a half-width of 4μm, which we suggest means the 1600 °C/Myr occurred around 450 °C, but the sample cooled faster at higher temperatures. We are currently exploring the relationships for Bishop Canyon, La Grange, and Seneca Township, all of which have reported measurements across a larger range of haf-widths. This will allow us to better constrain the thermal evolution, and thus physical structure, of the IVA meteorite parent body during cooling. In the future, we will also examine the extent to which other impacts that perturb the cooling history of a given parent body [e.g. 6] are recorded in the Widmanstätten pattern for a given sample.

References: [1] Yang et al. (2008) GCA 72, 3043-3061 [2] Hopfe and Goldstein (2001) MaPS 36, 135-154 [3] Dauphas (2007) MaPS 42, 1597-1613 [4] Crank (1984) Clarendon Press, 425 p. [5] Lyons et al. (2019) MaPS (Accepted) [6] Lyons et al. (2018) Goldschmidt, 1625